TU/e EINDHOVEN UNIVERSITY OF TECHNOLOGY

Electron density fluctuations in a dusty Ar/SiH4 rf discharge

Citation for published version (APA):
Stoffels, W. W., Stoffels, E., Kroesen, G. M. W., & Hoog, de, F. J. (1995). Electron density fluctuations in a dusty Ar/SiH4 rf discharge. *Journal of Applied Physics*, *78*(8), 4867-4872. https://doi.org/10.1063/1.359774

DOI:
10.1063/1.359774

Document status and date:
Published: 01/01/1995

Document Version:
Publisher's PDF, also known as Version of Record (includes final page, issue and volume numbers)

Please check the document version of this publication:

• A submitted manuscript is the version of the article upon submission and before peer-review. There can be important differences between the submitted version and the official published version of record. People interested in the research are advised to contact the author for the final version of the publication, or visit the DOI to the publisher's website.
• The final author version and the galley proof are versions of the publication after peer review.
• The final published version features the final layout of the paper including the volume, issue and page numbers.

Link to publication

General rights
Copyright and moral rights for the publications made accessible in the public portal are retained by the authors and/or other copyright owners and it is a condition of accessing publications that users recognise and abide by the legal requirements associated with these rights.

• Users may download and print one copy of any publication from the public portal for the purpose of private study or research.
• You may not further distribute the material or use it for any profit-making activity or commercial gain
• You may freely distribute the URL identifying the publication in the public portal.

If the publication is distributed under the terms of Article 25fa of the Dutch Copyright Act, indicated by the "Taverne" license above, please follow below link for the End User Agreement:

www.tue.nl/taverne

Take down policy
If you believe that this document breaches copyright please contact us at:

openaccess@tue.nl

providing details and we will investigate your claim.

Download date: 18. May. 2025

Electron density fluctuations in a dusty Ar/SiH_4 rf discharge

W. W. Stoffels,[a] E. Stoffels,[a] G. M. W. Kroesen, and F. J. de Hoog
Department of Physics, Eindhoven University of Technology, P.O. Box 513, 5600 MB Eindhoven, The Netherlands

(Received 13 March 1995; accepted for publication 27 June 1995)

The average electron density and electron density fluctuations in a dusty Ar/SiH_4 rf discharge have been studied using a microwave resonance technique. The average electron density increases with rf input power and it has a maximum as a function of pressure at about 30 mTorr. Within the first second of plasma operation the electron density decreases with a factor of ten. This is caused by submicroscopic particles, formed in the discharge, which rapidly absorb electrons. When the particles reach a critical size they are expelled from the plasma. This process is governed by a balance between the Coulomb force, trapping the particles in the positive plasma glow and the neutral drag force, flushing them out. The periodic growth and expulsion of particles, monitored by light scattering, results in an oscillatory behavior of the electron density. From the measured oscillation period (τ), which is in the order of seconds to minutes, and its dependence on the gas flow rate ($\mathcal{F}$) and on the fraction α of SiH_4 in the plasma ($\tau[\mathrm{s}] \approx 4.5 \times 10^2 \alpha^{-1} \mathcal{F}^{-2}$ [sccm], at 10 W rf power input), the trapping force (F_C) on particles can be calculated: $F_C[\mathrm{N}] \approx 4 \times 10^{-18} r$ [nm], where r is the radius of a particle. © *1995 American Institute of Physics.*

I. INTRODUCTION

Many investigators have been working on the problems related to dusty low pressure discharges[1,2] and significant progress has been made in understanding particle formation,[3] trapping,[4,5] charging[6] and transport.[7,8] Also the interaction of particles with the plasma has been studied.[9,10] In this paper we will discuss the behavior of the electron density in a dusty Ar/SiH_4 rf discharge. It has been shown that particle formation in this chemical system (under typical conditions: 5% SiH_4 in argon at 120 mTorr) is a three-step process.[3,11] Within several milliseconds after plasma ignition nanometer size particles are formed. In this process nearly all silicon in the gas phase is incorporated into these particles. In the next formation step these particles coalesce into structures of approximately 20 nm. At ambient temperature the coalescence phase lasts for about 50 ms. As the duration of this process is shorter than a typical residence time of species in the plasma (100 ms and longer), no new active gas is supplied and consequently the total particle mass remains constant during the coalescence. This implies that the particle density decreases. When the grain size reaches about 20 nm, the particles acquire a permanent negative charge and the repulsive Coulomb force prevents further coalescence. The negative charge traps the particles in the positive plasma glow, where they continue to grow by deposition of plasma species. This third formation phase lasts typically for several seconds. Afterwards the particles become too large, so they are (partly) expelled from the discharge and the cycle begins again. Such a formation mechanism results in homogeneously distributed particles with a well defined, monodisperse size distribution. However, several generations of monodisperse particles can be simultaneously present in the discharge.[3] Below we will show that the charging of particles results in a decrease of the electron density in the plasma during the particle formation. We will use this effect to monitor the particle growth and to determine the relative importance of the forces which trap the particles in the plasma.

II. EXPERIMENT

A detailed description of our experimental setup can be found elsewhere.[12,13] Briefly it consists of a capacitively coupled 13.56 MHz rf plasma confined in an aluminum cylinder (diameter: 175 mm, height: 50 mm). A scheme of the plasma box is given in Figure 1. The water cooled rf electrode (diameter: 120 mm) is part of the bottom of the cylinder, while the rest serves as a grounded electrode. Gas is introduced uniformly through the 2 mm wide slit between the rf and the grounded electrode. The top of the cylinder consists of a wire grid (grid size 0.5 mm), which enables a laminar gas flow through the plasma. Pressure and gas flow can be varied independently in the range of 1–1000 mTorr and 0–300 sccm, respectively. An automatic matching network optimizes the power dissipation in the plasma. The maximum power input is 120 W. Two vertical slits in the side walls of the plasma box allow to visualize particles by forward light scattering. In our case a He-Ne laser in combination with a monochromator and a photomultiplier is used.

The system is designed so the cylinder, formed by the electrodes, can simultaneously serve as a microwave cavity, which is used to determine the electron density in the plasma. A low power probing microwave is coupled into the cavity by means of an antenna and the resonance frequency is determined by tuning the microwave frequency to maximum transmission. The resonance frequency of the cavity (in our case about 3 GHz for the TM_{020} mode) depends on the electron density inside, so the latter can be determined from the shift of the resonance frequency with respect to its value in vacuum. This method provides a space averaged electron density, which can be monitored as a function of time with a resolution better than 100 ns. Further details about the method can be found in Ref. 12.

[a]Electronic mail: stoffels@discharge.phys.tue.nl

 0021-8979/95/78(8)/4867/6/$6.00 © 1995 American Institute of Physics

Downloaded 07 Jun 2010 to 131.155.151.122. Redistribution subject to AIP license or copyright; see http://jap.aip.org/jap/copyright.jsp

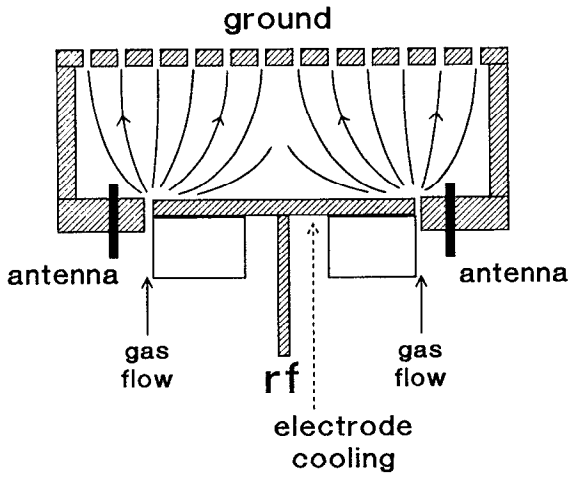

FIG. 1. A scheme of the electrode configuration. The direction of the gas flow is indicated.

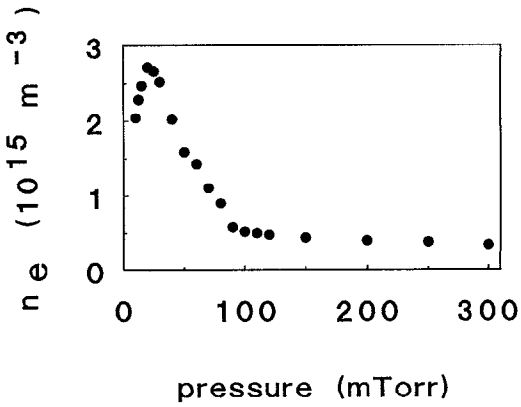

FIG. 3. The electron density as a function of pressure in an Ar/SiH_4 plasma. The gas mixture contains 5% SiH_4 in argon, the gas flow is 100 sccm and the rf power input is 10 W.

The geometry of our plasma box is similar to the one described by Boufendi and Bouchoule.[3,11] Only the gas flow in their configuration is directed downwards and injected through a shower head piece. Moreover, the electron densities, measured in these two systems under typical conditions for particle formation are the same.[14] Therefore it is expected that the particle growth kinetics in these two discharges is comparable.

III. RESULTS AND DISCUSSION

Some typical results of the electron density as a function of the rf power and pressure are shown in Figures 2 and 3. The data presented in these figures are time averaged values over minutes of plasma operation. In both cases the feed gas contains 5% SiH_4 in argon at a total flow rate of 100 sccm. It should be noted that the rf power input has been measured close to the generator and the power losses in the wires and the matching network are not subtracted. It is expected that these losses are a constant fraction of the total power, so the trends, shown in Figure 2, are correct.

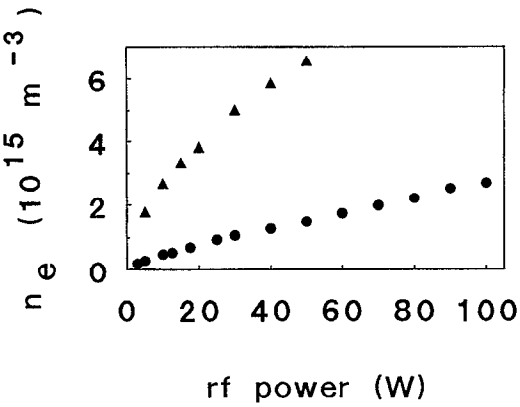

FIG. 2. The average electron density as a function of the rf power in an Ar/SiH_4 plasma. The pressure is 100 mTorr (dots) and 20 mTorr (triangle), the gas mixture contains 5% SiH_4 in argon and the gas flow is 100 sccm.

The pressure dependence of the electron density (Figure 3) is typical for an electronegative gas. Similar behavior has also been found in halocarbon (CF_4, CHF_3 and C_2F_6)[15] and oxygen rf discharges.[13] In the low pressure regime the electron density increases with pressure due to an increasing ionization frequency (increasing background gas density) and a decreasing loss rate of electrons to the wall. At higher pressures electron attachment becomes an important electron loss channel[16] and consequently the electron density decreases.

For pressures above 50 mTorr particle formation occurs, which can be visualized by forward laser light scattering. The formation and expulsion of particles result in periodic fluctuations of the electron density. The amplitude of these fluctuations decreases with increasing gas flow. Therefore the time averaged measurements of the electron density (Figures 2 and 3) have been performed at a relatively high flow rate (100 sccm).

At this flow rate the amplitude of the electron density fluctuations is only a few percent of the total electron density. For lower flow rates the electron density fluctuations reach up to 50% of the total electron density. The time averaged electron density is only weakly flow dependent; typically it increases 5 to 10% with increasing flow in the range from a few to 300 sccm.

Figure 4 shows the time evolution of the electron density after the plasma has been switched on. The electron density is high immediately after switching on the discharge and it decreases rapidly during the first 100 ms of plasma operation. This feature is not present in an argon plasma, where a small transient peak in the electron density, caused by an overshoot of the rf generator, disappears within tens of microseconds. The observed time scale for the electron density decrease in an Ar/SiH_4 plasma corresponds with the typical time scale for the coalescence of the first crystallites.[3] After the clusters are formed, the electron density increases slightly again. Similar behavior has been observed in a dusty Ar/CCl_2F_2 plasma,[12,17] but in the latter case the amplitude of the fluctuations is lower and the time constant is much longer. The long term behavior of the electron density depends on the gas flow: at 300 sccm a steady state is reached

Downloaded 07 Jun 2010 to 131.155.151.122. Redistribution subject to AIP license or copyright; see http://jap.aip.org/jap/copyright.jsp

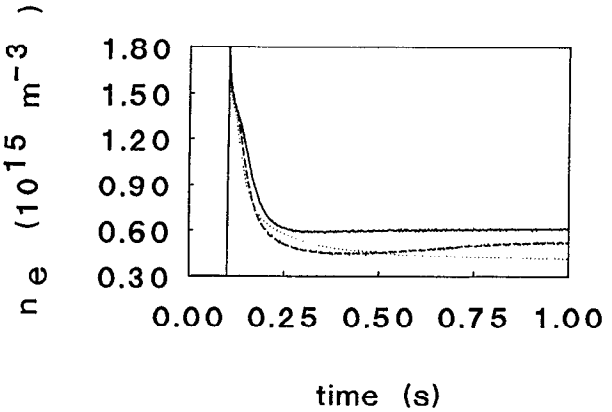

FIG. 4. Time behavior of the electron density after switching the discharge on for three different flow rates: 300 sccm—solid curve, 100 sccm—dashed curve and 30 sccm—dotted curve. The gas mixture contains 5% SiH_4 in argon, the pressure is 120 mTorr and the rf power is 20 W.

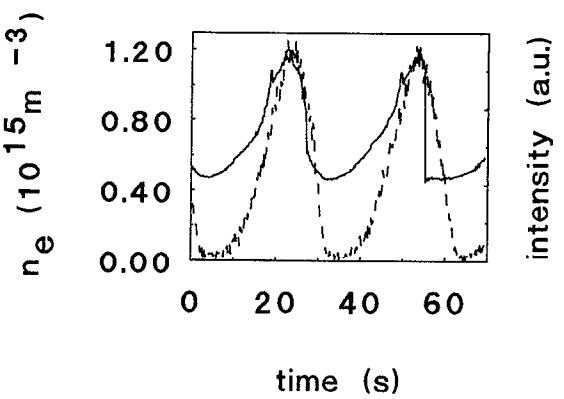

FIG. 6. The time dependent He-Ne scattering signal (forward scattering at 5° from particles that flushed out of the discharge through the vertical slits in the cavity, dashed curve) and the electron density (solid curve). The gas mixture contains 5% SiH_4 in argon, the pressure is 120 mTorr, the gas flow is 15 sccm and the rf power is 10 W.

after 200–300 ms. At 100 sccm only small variations in the electron density are observed after 1 s of plasma operation. At low flows (≤30 sccm) a stationary state is never reached and the plasma exhibits a periodic behavior. This is shown in Figure 5, where the electron density fluctuations during the first 18 s of plasma operation are shown. It should be mentioned that these oscillations do not damp and can last from minutes to hours. Furthermore they are very well reproducible. As mentioned before, the fluctuations in the electron density are caused by a periodic growth and expulsion of particles in the discharge. Because the particles efficiently absorb electrons, the electron density decreases during particle formation. In Figure 6 the scattered laser light from particles, leaving the discharge through the vertical slits in the cavity, is shown together with the electron density fluctuations. In Figure 6 a high electron density coincides with a high scattering signal *outside* the cavity. At this moment, the actual particle density *inside* the cavity is low, as the particles have been expelled. The phase shift between the scattering signals inside and outside the cavity is shown in Figure 7. Unfortunately, the geometry of the cavity does not allow to obtain a scattering signal solely from inside the cavity.

The electron current to the particles is balanced by a positive ion current. Thus in presence of particles the ion losses are enhanced, while on the other hand there are less electrons to maintain the ionization. This has to be compensated by an increase of the average electron energy. Bouchoule and Boufendi[18] have shown by means of optical emission spectroscopy that the electron excitation temperature increases significantly in presence of particles. Also in our case a notable *increase* of the optical emission intensity from the discharge has been observed in the course of particle formation, even though the electron density decreases during this process.

It is clear that a negatively charged particle is trapped in the plasma glow, because the Coulomb force prevents it from entering the plasma-sheath boundary. However, a good evaluation of the magnitude of this force needs a careful

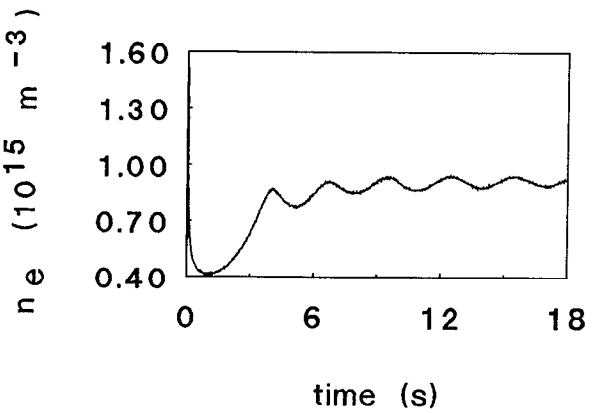

FIG. 5. Time behavior of the electron density after switching the discharge on. The gas mixture contains 5% SiH_4 in argon, the pressure is 120 mTorr, the gas flow is 30 sccm and the rf power is 20 W. The fluctuations continue without damping for minutes up to hours.

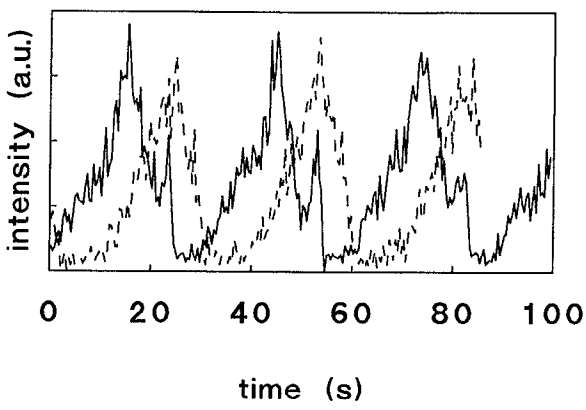

FIG. 7. The scaled time dependent He-Ne scattering signals from particles inside (solid curve) and outside (dashed curve) the discharge for the conditions of Figure 6. The delay between the two curves indicates the time needed to transport the particles out of the plasma. Due to limited optical access to the cavity, the solid curve is partly influenced by scattering on particles outside the cavity.

Downloaded 07 Jun 2010 to 131.155.151.122. Redistribution subject to AIP license or copyright; see http://jap.aip.org/jap/copyright.jsp

approach. In the glow particles can move relatively freely, because the dc electric fields are small. Only at high particle densities collective effects are important and Coulomb liquids or solids are formed. Here we consider a plasma containing only isolated particles. In this case the negative charge on each particle is shielded by a surrounding local positive space charge. Consequently, in the glow the particle surrounded by its positive cloud forms a quasi-neutral system, on which only weak polarization forces act. The actual number of electrons on a particle (Q) is determined by a balance between the electron (Φ_e) and the ion flux (Φ_+) towards the particle surface. A simple model for particles smaller than the Debye length yields:[12,19]

$$\Phi_e = 2\sqrt{\frac{2\pi k_b T_e}{m_e}}\, n_e r^2 \exp\left(-\frac{q^2 Q}{4\pi\epsilon_0 r k_b T_e}\right),$$
$$\Phi_+ = 2\sqrt{\frac{2\pi k_b T_+}{m_+}}\, n_+ r^2 \left(1+\frac{q^2 Q}{4\pi\epsilon_0 r k_b T_+}\right). \quad (1)$$

Here $T_{e,+}$, $m_{e,+}$ and $n_{e,+}$ are the electron and ion temperatures, masses and densities; q, k_b and ϵ_0 are the elementary charge, the Boltzmann constant and the electric permittivity in vacuum; r is the particle radius. From the above expressions it follows that the charge on a particle is proportional to its radius. Moreover, it depends on the local plasma parameters, especially on the ratio of the electron to ion density. For typical rf plasma conditions: $n_e = 10^{15}$ m^{-3}, $n_+ = 10^{16}$ m^{-3}, $T_e = 3$ eV and $T_+ = 350$ K, the model yields: $Q = 2\,r$ (Q in elementary charges and r in nanometers). Furthermore the model predicts that the charging time for an initially neutral particle is inversely proportional to the particle radius. For the plasma parameters given above τ_C [s] $= 6 \times 10^{-4}/r$ [nm]. However, these parameters can show significant spatial variations, especially in the sheath. In this region also the positive space charge around the particle deforms under influence of the strong electric fields and the plasma density gradients. These electric fields are poorly known and possibly affected by the presence of particles. Therefore, a simple analytical expression for the Coulomb force at the plasma boundary cannot be obtained. So far only extensive particle-in-cell and fluid codes have been applied to tackle this problem.[20–22] However, in any case the Coulomb force is proportional to the particle charge and thus to its radius.

Other possibly important forces acting on the particles are: the neutral drag force F_n, the ion drag force F_i, the thermophoretic force F_{th} and the gravitational force F_g. They can be estimated by[1,12]:

$$F_n = \tfrac{4}{3}\pi r^2 n_g v_g m_g v_{th} \approx 5\times 10^{-16}\ \text{N} \quad (2)$$

$$F_i = K_{mt} n_+ m_+ v_{+d} \approx 10^{-15}\ \text{N (in the sheath}^{21,23}\text{)} \quad (3)$$

$$F_{th} = \frac{3\pi r^2 p \lambda \nabla T}{2T} \approx 10^{-16}\ \text{N} \quad (4)$$

$$F_g = \tfrac{4}{3}\pi r^3 \rho g \approx 10^{-16}\ \text{N}. \quad (5)$$

The estimates given above are made for a gas pressure p of 120 mTorr and a gas flow $\mathcal{F}$ of 30 sccm, so the gas density and velocity are $n_g = 3.6\times 10^{21}$ m^{-3} and $v_g = 0.2$ m/s. The particle radius $r = 100$ nm, the mass of an Ar atom $m_g = 40$ amu, the thermal gas velocity $v_g = 300$ m/s, the mean free path of neutrals $\lambda = 5\times 10^{-4}$ m, the temperature $T = 300$ K, with a gradient $\nabla T = 10^2$ K/m, the specific particle density $\rho = 2\times 10^3$ kg/m^3 and the gravitational constant $g = 9.81$ m/s^2. K_{mt} denotes the rate coefficient for ion momentum transfer ($K_{mt} \approx 10^{-5}$ m^3/s); m_+ and v_{+d} are the positive ion mass and drift velocity. As the dc electric field in an electronegative plasma is negligible, the ion drift velocity is small except for the sheath region. Therefore, the ion drag force is only important near the sheath region. Space resolved line broadening measurements by means of infrared absorption spectroscopy have shown that there is no significant temperature gradient in our plasma, thus the thermophoretic force is not very important. It has however the same r^2 dependence on radius as the neutral drag force. Consequently, in the plasma glow the most important force is the neutral drag force, which flushes the particles out of the plasma glow. Once the particles are pushed into the (pre)sheath, where the directed ion flux exceeds the random ion flux, the ion drag force can also become significant. At the same time the charge on a particle can decrease due to the lower electron to positive ion density ratio in the sheath [see Equation (1)]. This diminishes the repulsive Coulomb force, allowing the particles to be pushed towards the electrodes, or in our case, to be expelled from the discharge through the wire grid on top of the plasma box. Even if in this last stage the ion drag force is dominant, it is the neutral drag force which initiates the expulsion of the particles from the plasma glow.

The neutral drag force [Equation (2)] is proportional to the particle cross section (πr^2), the directed flux of gas atoms or molecules hitting the particle ($n_g v_g$) and the momentum transfer per collision ($m_g v_{th}$). As $n_g v_g$ is proportional to the gas flow rate ($\mathcal{F}$), it is clear that the neutral drag force scales as $F_n \sim r^2 \mathcal{F}$. This implies that the neutral drag force is independent of pressure at a constant non-turbulent gas flow. As the neutral drag force grows with the square of the particle radius whereas the Coulomb force is only proportional to the radius, the particles will be expelled from the plasma glow after they have reached a critical size. Below we will use the average neutral drag force, assuming a homogeneous, laminar flow through the plasma volume. This accurately describes the flushing out of particles, but it is strictly speaking not correct for the lower region of the plasma near the gas inlet and the rf electrode (see Figure 1).

Using SEM pictures Boufendi and Bouchoule[3] have shown that the particle radius increases linearly with time within the first seconds after the start of particle nucleation, in their case after plasma ignition. The particle radius is also proportional to the amount of SiH_4 introduced into the discharge ($\mathcal{F}_{SiH_4}$).[24] The latter can be varied by changing the fraction of SiH_4 in the gas mixture (α) or by changing the total flow. Thus $\mathcal{F}_{SiH_4} = \alpha\mathcal{F}$. At a given time τ (the oscillation period) a critical radius is reached, for which the Coulomb force is balanced by the neutral drag force. By introducing $r \sim \mathcal{F}_{SiH_4}\tau$ into the force balance and remembering that $F_C \sim Q \sim r$ we obtain:

$$F_C = F_n \Rightarrow r \sim r^2 \mathcal{F} \Rightarrow \mathcal{F}_{SiH_4}\mathcal{F}\tau = \text{const} \Rightarrow \alpha \mathcal{F}^2 \tau = \text{const}.$$

Downloaded 07 Jun 2010 to 131.155.151.122. Redistribution subject to AIP license or copyright; see http://jap.aip.org/jap/copyright.jsp

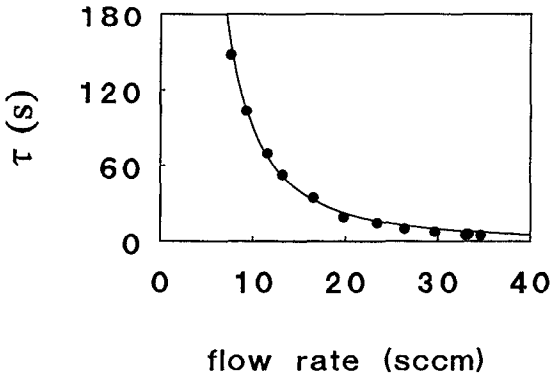

FIG. 8. The period of the electron density fluctuation as a function of the gas flow rate ($\mathcal{F}$). The gas mixture contains 5% SiH_4 in argon, the pressure is 120 mTorr and the rf power is 10 W. The curve represents a fitted $\mathcal{F}^{-2}$ dependence.

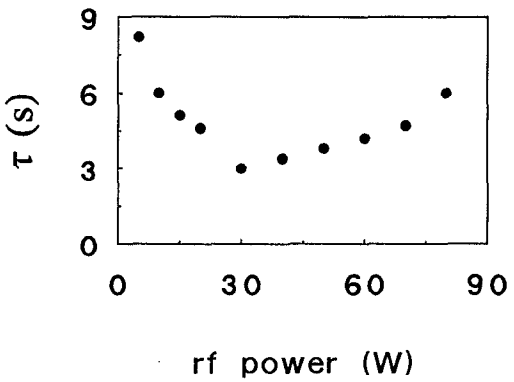

FIG. 10. The period of the electron density fluctuation as a function of the rf power. The gas mixture contains 5% SiH_4 in argon, the pressure is 120 mTorr and the total gas flow is 30 sccm.

Consequently, the oscillation period is inversely proportional to the fraction of SiH_4 in the feed gas and the square of the total gas flow rate:

$$\tau = \frac{C}{\alpha \mathcal{F}^2}, \tag{6}$$

where C is a constant.

The period of the electron density fluctuations as a function of the gas flow in a 5% SiH_4 gas mixture is shown in Figure 8. The data points are fitted using Equation (6), derived from the balance of electric and neutral drag forces. Also the predicted inverse proportionality of the oscillation period with the fraction of SiH_4 in the feed gas (α) is observed experimentally (Figure 9). It is clear that the experimental data agree very well with the proposed mechanism of particle expulsion from the plasma by the neutral drag force. From these data the constant C in Equation (6) is found: $C \approx 4.5 \times 10^2$ [s sccm^2], with τ in seconds and $\mathcal{F}$ in sccm. In the following we will assume that the growth rate of our particles is almost indentical to the one measured by Boufendi and Bouchoule:[3]

$$r \approx 7 \alpha \mathcal{F} t \tag{7}$$

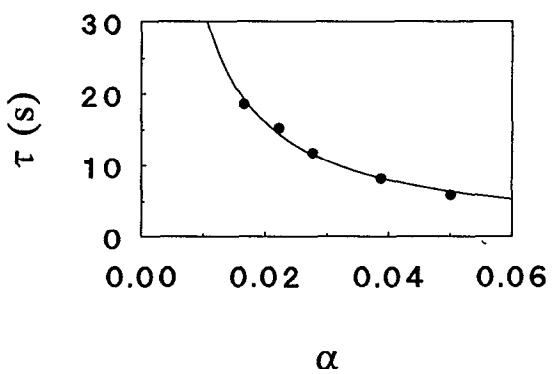

FIG. 9. The period of the electron density fluctuation as a function of the fraction SiH_4 in the gas mixture (α). The pressure is 120 mTorr, the rf power is 10 W and the total gas flow is 30 sccm. The curve represents a fitted α^{-1} dependence.

where the particle radius r is in nanometers and t [s] denotes the plasma operation time. This seems a valid assumption as the plasma reactors and conditions are comparable. Using this growth rate, Equation (2) and the experimentally determined oscillation period in Equation (6), we can evaluate the critical force needed to expel a particle from the plasma glow:

$$F_C \approx 4 \times 10^{-18} r \tag{8}$$

where the force is given in Newton and the particle radius in nanometers.

At constant gas flow no pressure dependence of the oscillation period has been observed. This agrees with the proposed mechanisms of particle growth and expulsion. The oscillation period does depend however on the rf power input in the discharge, as shown in Figure 10. There is a minimum in the oscillation period at about 30 W. The increase at low rf powers is probably caused by lower chemical activity of the plasma (low electron density, see Figure 2). This results in a reduced particle growth rate and consequently in a longer oscillation period. At intermediate rf powers the conditions for particle formation are optimal. For high powers it can be expected that the effective particle growth rate is reduced due to an increasing ion bombardment (etching). Furthermore, the electric fields are higher under these conditions, which increases the Coulomb force, trapping the particles in the discharge. Both factors result in an increase of the oscillation period at higher rf powers.

IV. CONCLUSIONS

Particle formation has a large influence on all plasma parameters. Therefore the presence and growth of particles can be studied indirectly by monitoring changes in several plasma parameters. The change in the electron density is a good indication of the presence of particles, as the latter very efficiently attach electrons, become negatively charged and form important recombination sites. A significant decrease of the electron density during particle formation has been observed. The particles are trapped in the plasma by the Cou-

Downloaded 07 Jun 2010 to 131.155.151.122. Redistribution subject to AIP license or copyright; see http://jap.aip.org/jap/copyright.jsp

lomb force and can be expelled by the neutral drag force. As the latter increases quadratically with the particle size while the former is only linear with size, there is a maximum size for particles in the plasma. When particles reach this size they are expelled from the plasma and a new particle generation can be formed. This results in a periodic behavior of the plasma, which is reflected by oscillations of the electron density. The period depends on the particle growth rate and the magnitude of forces acting on a particle. The experimentally determined dependencies of the oscillation period on external plasma parameters (flow rate, feed gas composition, pressure and rf power) can be predicted by considering a force balance between the Coulomb and the neutral drag force.

ACKNOWLEDGMENT

This work has been supported by the BRITE-EURAM programme of the European Community under project N^0 7328 and contract BRE2-CT94-0944.

[1] Nato Advanced Workshop on the Formation, Transport and Consequences of Particles in Plasmas, Chateau de Bonas, Castéra-Verduzan, France, Aug., Sept. 1993, pp. 239–451; Plasma Sources Sci. Technol. **3**, 3 (1994).
[2] Special issue on charged dust in plasmas. IEEE Trans. Plasma Sci. **22**, 89 (1994).
[3] L. Boufendi and A. Bouchoule, Plasma Sources Sci. Technol. **3**, 262 (1994).
[4] R.N. Carlile, S. Geha, J.F. O'Hanlon, and J.C. Stewart. Appl. Phys. Lett. **59**, 1167 (1991).
[5] G.S. Selwyn, J.E. Heidenreich, and K.L. Haller, J. Vac. Sci. Technol. A **9**, 2817 (1991).
[6] J. Goree, Plasma Sources Sci. Technol. **3**, 400 (1994).
[7] D.J. Rader and A.S Geller, Plasma Sources Sci. Technol. **3**, 426 (1994).
[8] S.E. Beck, S.M. Collins, and J.F. O'Hanlon, IEEE Trans. Plasma Sci. **22**, 128 (1994).
[9] J.P. Boeuf, Ph. Belenguer, and T. Hbid, Plasma Sources Sci. Technol. **3**, 406 (1994).
[10] G.M. Jellum and B.D. Graves, J. Appl. Phys. **67**, 6490 (1990).
[11] L. Boufendi, J. Hermann, A. Bouchoule, B. Dubreuil, E. Stoffels, W.W. Stoffels, and M.L. De Giorgi, J. Appl. Phys. **76**, 148 (1994).
[12] E. Stoffels and W.W. Stoffels, Ph.D thesis, Eindhoven University of Technology, 1994.
[13] E. Stoffels, W.W. Stoffels, D. Vender, M. Kando, G.M.W. Kroesen, and F.J. de Hoog, Phys. Rev. E **51**, 1224 (1995).
[14] L. Boufendi, T. Hbid, F. Vivet, P. Lefaucheux, and A. Bouchoule. *Europhysics Conference Abstracts 18E, ESCAMPIG 94. 79*, edited by M.C.M. Van de Sanden (European Physical Society, Eindhoven, The Netherlands, 1994).
[15] M. Haverlag, A. Kono, D. Passchier, G.M.W. Kroesen, W.J. Goedheer, and F.J. de Hoog, J. Appl. Phys. **70**, 3472 (1991).
[16] D. Vender, W.W. Stoffels, E. Stoffels, G.M.W. Kroesen, and F.J. de Hoog, Phys. Rev. E **51**, 1236 (1995).
[17] E. Stoffels, W.W. Stoffels, W.W. J. Appelman, G.M.W. Kroesen, and F.J. de Hoog, *Proceedings of the 11th International Symposium on Plasma Chemistry*, edited by J.E. Harry (International Organizing Committee of ISPC-11, Loughborough, UK, 1993), Vol. 4, p. 1528.
[18] A. Bouchoule and L. Boufendi, Plasma Sources Sci. Technol. **3**, 292 (1994).
[19] R.N. Nowlin and R.N. Carlile, J. Vac. Sci. Technol. A **9**, 2825 (1991).
[20] S.J. Choi and M.J. Kushner, IEEE Trans. Plasma Sci. **22**, 138 (1994).
[21] D.B. Graves, J.E. Daugherty, M.D. Kilgore, and R.K. Porteous, Plasma Sources Sci. Technol. **3**, 433 (1994).
[22] J.P. Boeuf, Phys. Rev. A **46**, 7910 (1992).
[23] J. Perrin, P. Molinas-Mata, and P. Belenguer, J. Phys. D: Appl. Phys. **27**, 2499 (1994).
[24] L. Boufendi and A. Bouchoule (unpublished data).

Downloaded 07 Jun 2010 to 131.155.151.122. Redistribution subject to AIP license or copyright; see http://jap.aip.org/jap/copyright.jsp